

# Quantum signature of a period-doubling bifurcation and scars of periodic orbits

C. P. Malta

*Instituto de Física, Universidade de São Paulo, Caixa Postal 20516, 01498-970 São Paulo, São Paulo, Brazil*

M. A. M. de Aguiar and A. M. Ozorio de Almeida

*Instituto de Física, Universidade de Campinas, Caixa Postal 6165, 13081-970 Campinas, São Paulo, Brazil*

(Received 23 April 1992)

The density of states is numerically calculated for a nonintegrable Hamiltonian whose shortest-periodic-orbit family undergoes a period-doubling bifurcation in the energy interval considered. Smoothing the density using a suitable width  $\delta E$ , oscillations are observed due to only the family of shortest periods or also its period doubling. The period-doubling resonance results in a higher average amplitude of the corresponding spectral oscillations than for the primitive orbit. The main periodic families produce strong scars in the wave intensities. Projections of the Husimi distributions also exhibit scars that are, however, not so clear.

PACS number(s): 03.65.Sq, 05.45.+b

## I. INTRODUCTION

In the past two decades a great amount of work has been done to understand the implications of the Gutzwiller trace formula [1] in a number of situations. The main difficulty resides in the intrinsic structure of the trace formula, which connects the semiclassical density of states to a sum over all the periodic orbits of the associated classical problem. If the exact spectrum is usually difficult to obtain, so is the totality of the classical periodic orbits. The influence of the periodic orbits in the eigenstates seems to be even more complex. Scars were first reported by Heller [2] in the individual eigenstates of the Bunimovich billiard, and a theory was proposed in terms of the averaged local density of states [3]. More accurate results were then obtained by Bogomolny [4] for the probability density in the coordinate representation. Finally, Berry [5] lifted the results of Bogomolny to the phase space via the Wigner function. All of these theories, however, rely strongly on energy averages, and do not apply to individual states. It is therefore important to provide numerical examples of the scarring effect to guide the development of theories.

We consider here a smooth, nonintegrable, Hamiltonian ("soft chaos") in contrast to the existing studies that refer to billiards and/or systems exhibiting a symbolic code for their periodic orbits. In the extreme case of a separable Hamiltonian, the Gutzwiller formula can be shown to agree with the Einstein-Brillouin-Keller torus quantization conditions [6], which greatly simplifies the calculations. However, in the general nonintegrable case, where chaos and tori are intermixed, the only known way to overcome the classical complexity is by smoothing [7] the density of states. This procedure, although poorer in resolution, opens the possibility of cutting off the contribution of long periodic orbits, leading to a more treatable trace formula.

In this paper we investigate, numerically, the smoothed density of states for the smooth, nonintegrable, Hamil-

tonian

$$H = (p_x^2 + p_y^2)/2 + V(x, y), \quad (1)$$

with

$$V(x, y) = (y - x^2/2)^2 + 0.05x^2. \quad (2)$$

The simplest periodic orbits of this system have been extensively studied by Baranger and Davies [8]. This potential (named NELSON) has a minimum at zero energy, and due to the reflexion symmetry in both  $x$  and  $p_x$ , the plane  $x=0$ ,  $p_x=0$  is an invariant plane in the phase space. Since the potential is harmonic along this plane, it is foliated by a family of "vertical" ( $y$  direction) oscillations of constant period  $\tau = 2\pi/\sqrt{2}$ . According to the numerical study of Baranger and Davies [8], this is the family of orbits with the shortest period in the energy interval (0.0, 0.300). In this interval, the vertical family undergoes three main bifurcations: a period-quadrupling at  $E \approx 0.019$ , a period-tripling at  $E \approx 0.077$ , remaining elliptic in both cases, and finally, a period-doubling at  $E \approx 0.136$ , then becoming weakly hyperbolic. (We shall call these bifurcated families V4, V3, and V2, respectively.) These families have the shortest periods in the above-mentioned energy interval. Another important family of this system is the "horizontal" family, so called because it starts out as a harmonic oscillation in the  $x$  direction. Its period is always greater than the period of V4, and in that energy interval it undergoes two consecutive isochronous bifurcations [8,9], one of the generated families being elliptic.

Our purpose in this paper is to identify the signature of some of these families in the quantum spectrum and eigenfunctions, including the classical phenomenon of bifurcation. This will be done by controlling the smoothing of the spectral density, as in the previous work of Malta and Ozorio de Almeida [10]. We also present the Husimi distributions projected on both  $(x, p_x)$  and  $(y, p_y)$  planes. These projections may provide information about the

scarred states but, in order to obtain fine details, a long computation time is required. The wave intensities, on the other hand, can be calculated with very good precision and much less effort.

This paper is organized as follows. In Sec. II we present the smoothed density of states and show the signature of the classical orbits and bifurcations in its (discrete) Fourier transform, using Gaussian windows [11]. In Sec. III we show scars of periodic orbits in the averaged wave intensities and in the Husimi distributions. The conclusion is given in Sec. IV.

## II. THE SMOOTHED DENSITY OF STATES

The eigenvalue problem of the NELSON quantum system,

$$H\psi_i(x,y) = E_i\psi_i(x,y),$$

was solved using the expansion

$$\psi_i(x,y) = \sum_{n=0}^M \sum_{n=0}^N C_i^{n,N-n} \phi_n(x) \phi_{N-n}(y), \quad (3)$$

where  $\phi_n(x)$  and  $\phi_m(y)$  are the eigenfunctions of the one-dimensional harmonic-oscillator Hamiltonians  $H_x$  and  $H_y$ ,

$$H_x = p_x^2/2 + 0.05x^2, \quad H_y = p_y^2/2 + y^2. \quad (4)$$

The prime in the summation meaning that only even  $n$  (even parity) or only odd  $n$  (odd parity) are included.

The truncation value  $N=M$ , in the expansion (3), is chosen according to the energy interval to be investigated, for a given  $\hbar$ . Semiclassical results are obtained by using a small  $\hbar$ , and for a given energy interval, the smaller  $\hbar$  is, the larger  $M$  has to be. We used  $M=118$  and diagonalized a matrix  $3600 \times 3600$ . The calculation has been done for  $\hbar=6.0 \times 10^{-3}$  and  $9.0 \times 10^{-3}$ , for which the level spacing of the vertical harmonic oscillator,  $\hbar\omega_y$ , is approximately  $8.5 \times 10^{-3}$  and  $12.7 \times 10^{-3}$ , respectively. For the truncation value used, the eigenvalues contained in the energy interval (0,0.200) are good. The corresponding eigenfunctions are fairly good for the larger value of  $\hbar$  used, but are not so good for the smaller value (of course, the lower the eigenvalue, the better the corresponding eigenfunction).

The density of states (histograms), as a function of the energy  $E$ , has been calculated in the above energy interval, with various degrees of smoothing. These densities have been Gaussian smoothed, with half width  $\delta E$ , in order to eliminate spurious fluctuations that arise when the number of states contained in  $\delta E$  is small.

According to the periodic orbit theory, the density of states may be separated in two terms [12],

$$d(E) = d_{av}(E) + d_{osc}(E), \quad (5)$$

where  $d_{av}(E)$  is the average density of states (the so-called Weyl term) corresponding to zero period orbits, and  $d_{osc}(E)$  is the oscillatory term which incorporates the contribution of the periodic orbits of period greater than zero. The contribution to  $d_{osc}(E)$  of the lowest period orbits may be analyzed numerically by appropriately choos-

ing the value of  $\delta E$  used in the calculation. As the vertical family has the lowest period,  $d_{osc}(E)$  will exhibit no oscillations, as  $\hbar \rightarrow 0$ , if  $\delta E > \hbar$  ( $\omega_y = \sqrt{2}$ ) (for small values of  $\hbar$ , there will be no oscillations only if  $\delta E$  is fairly larger than  $\hbar\omega_y$ ). In order to observe the contribution of the periodic family V2, resulting from a period-doubling bifurcation of the vertical family,  $\delta E$  must be smaller than  $\hbar\omega_y/2$ . For  $\delta E$  slightly smaller than  $\hbar\omega_y/4$ , in the energy interval under consideration,  $d_{osc}(E)$  will have contributions of the vertical family and of all the periodic families resulting from a period- $n$  (period-2 denotes doubling, period-3 denotes tripling, etc.) bifurcation,  $n \leq 4$ , of this vertical family, i.e., families V2, V3, and V4.

The smoothed level densities  $d(E)$ , for  $\hbar=6.0 \times 10^{-3}$  and  $9.0 \times 10^{-3}$ , were calculated using, respectively,  $\delta E=1.0 \times 10^{-3}$  and  $2.0 \times 10^{-3}$ . It should be mentioned that these densities were obtained numerically, at energy points separated by  $\varepsilon=1.0 \times 10^{-4}$  and, in all the figures below, a line was drawn joining consecutive points.

The term  $d_{osc}(E)$  is obtained by subtracting the Weyl term  $d_{av}(E)$  from the level density  $d(E)$ . The Weyl term has been obtained numerically, using  $\delta E=40.0 \times 10^{-3}$  (see Fig. 1). It should be mentioned that, for the NELSON potential, the Weyl term may be calculated analytically and it is a linear function of  $E$  [in fact, this linear behavior of  $d_{av}(E)$  is used to verify the appropriateness of the truncation value  $N=M$  for the energy interval under investigation], but we have preferred to use the numerical result for numerical consistency reason. The ratio of the angular coefficients of the  $d_{av}(E)$  terms displayed in Fig. 1 is equal to the ratio of the corresponding  $\hbar^{-2}$ , in agreement with the analytical result.

In Figs. 2(a) and 2(b) we display the term  $d_{osc}(E)$ , obtained by subtracting the corresponding Weyl term in Fig. 1, from the corresponding  $d(E)$ . In the semiclassical periodic orbit theory, the oscillations exhibited by  $d_{osc}(E)$  in Figs. 2(a) and 2(b), should be due to the contributions of the periodic orbits with periodic up to  $2\pi\hbar/\delta E$ . The  $\delta E$  value used, for both values of  $\hbar$ , is smaller than  $\hbar\omega_y/4$ , therefore, the vertical orbit and the orbits of V2, V3, and V4 (plus all their  $m$ th repetitions for which

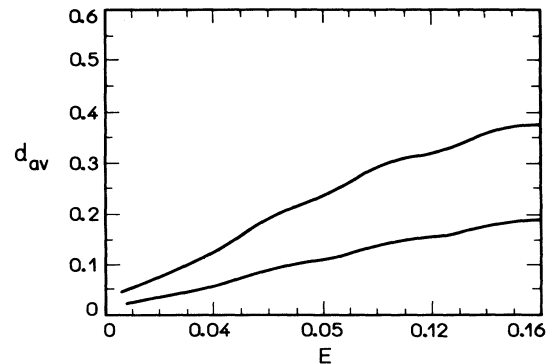


FIG. 1. The Weyl term  $d_{av}(E)$  for  $\hbar=6.0 \times 10^{-3}$  (steeper curve) and for  $\hbar=9.0 \times 10^{-3}$  (the oscillations are due to the Gaussian smoothing).

$m\tau \leq 2\pi\hbar/\delta E$ ) should be contributing to those oscillations. In the energy region after the period-doubling bifurcation has occurred, the main contribution should come from V2, as the vertical orbit becomes hyperbolic after this. Nevertheless, the contribution of the vertical orbit remains significant even after its period-doubling bifurcation, because its instability sets in very slowly. The contributions of V3 and V4 are not so significant since, as already mentioned, the vertical orbit remains stable at those bifurcations.

In order to verify all those facts mentioned above, we made a Fourier analysis of  $d_{\text{osc}}(E)$  in Figs. 2(a) and 2(b), using Gaussian windows [11]. Considering the whole energy interval (a single window), the Fourier analysis

$$F(\nu_k) = \sum_{n=0}^{N-1} W(n) d_{\text{osc}}(n\varepsilon) \exp(-2\pi i \nu_k n\varepsilon),$$

$$\nu_k = k/(N\varepsilon), \quad k=0, \dots, N-1$$

with the Gaussian window [11]

$$W(n) = \exp[-18.0(n/N)^2],$$

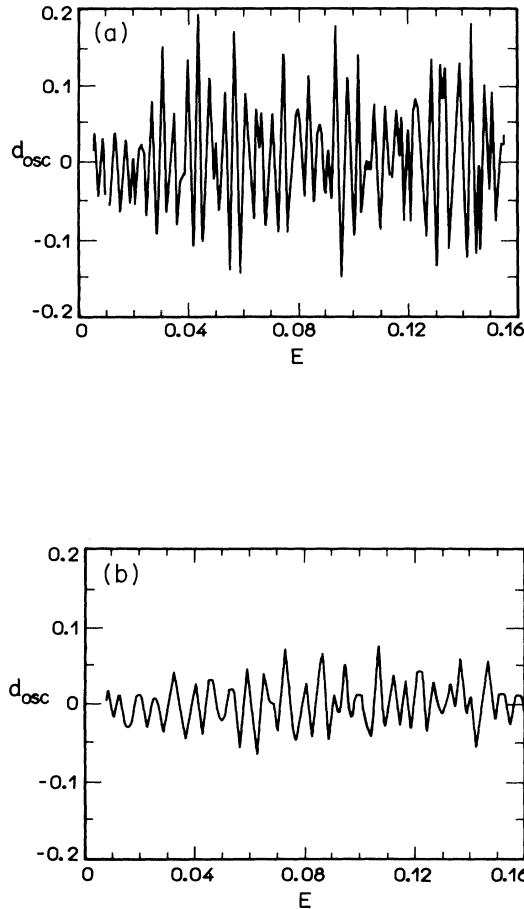


FIG. 2. (a)  $d_{\text{osc}}(E)$  for  $\hbar=6.0 \times 10^{-3}$ , using  $\delta E=1.0 \times 10^{-3}$ . (b)  $d_{\text{osc}}(E)$  for  $\hbar=9.0 \times 10^{-3}$ , using  $\delta E=2.0 \times 10^{-3}$ . One should note that  $\tau_{\text{max}}=2\pi\hbar/\delta E$  is smaller here than in (a) resulting in the smaller frequency and amplitude of the fluctuations.

shows that, in both cases, the main frequency contributing is  $2(\hbar\omega_y)^{-1}$ , but the frequency  $(\hbar\omega_y)^{-1}$  still contributes significantly. This is displayed in Figs. 3(a) and 3(b), where we plot  $|F(\nu)|^2 \times \nu$ . As for the frequencies  $3(\hbar\omega_y)^{-1}$  and  $4(\hbar\omega_y)^{-1}$ , their contributions are small, as expected [it should be mentioned that the single window Fourier analysis does not exhibit peaks at these frequencies if  $(\hbar\omega_y/3) < \delta E < (\hbar\omega_y/2)$ ]. The contribution of the horizontal family ( $\nu \in [535, 555]$  for  $\hbar=6.0 \times 10^{-3}$ ,  $\nu \in [357, 370]$  for  $\hbar=9.0 \times 10^{-3}$ ) is also very small.

It is easy to calculate the amplitude of the oscillations for each of the periodic orbits viewed through the Gaussian window employed in analyzing the spectrum. Figure 4 shows the Gutzwiller amplitude

$$\frac{\tau}{\{\sin[\vartheta(E)/2]\}^{1/2}}$$

for V, 2V, and V2, where  $\vartheta(E)$  is the stability angle of the orbit. The amplitude of the second repetition of the V orbit exhibits a singular peak at the period-doubling bifur-

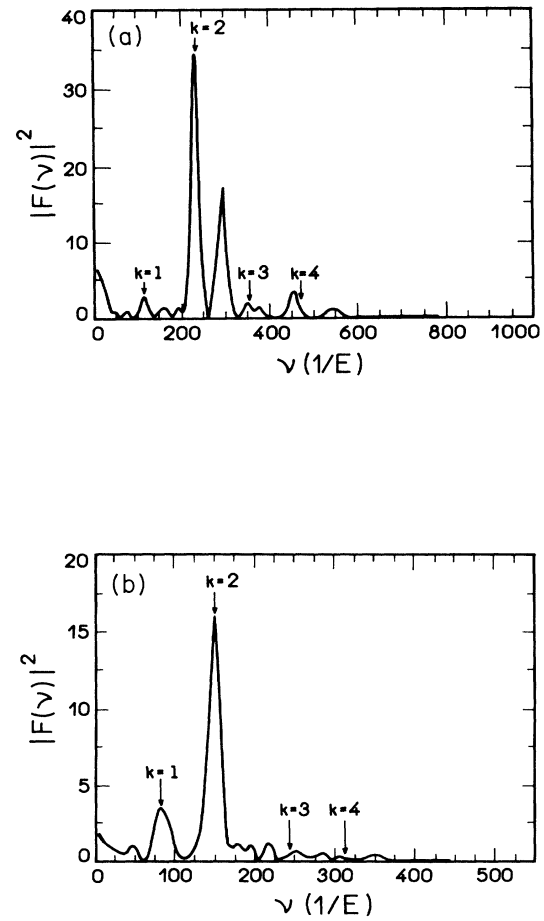


FIG. 3. (a) Single Gaussian window Fourier analysis of  $d_{\text{osc}}(E)$  in Fig. 2(a). The arrows indicate the frequencies  $k(\hbar\omega_y)^{-1}$ ,  $k=1,2,3$ . (b) Single Gaussian window Fourier analysis of  $d_{\text{osc}}(E)$  in Fig. 2(b). The arrows indicate the frequencies  $k(\hbar\omega_y)^{-1}$ ,  $k=1,2,3$ .

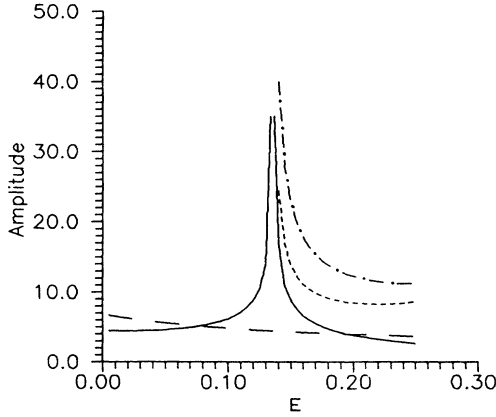


FIG. 4. The Gutzwiller amplitudes. The continuous line is the second repetition of V (2V), long dash is V, short dash is V2, and dot-dash is the sum of V2 and 2V.

cation point ( $E \approx 0.136$ ). The theory of Ozorio de Almeida and Hannay [13] substitutes this singularity by a finite peak, but the general picture is the same. It is, therefore, satisfying that Figs. 2(a) and 2(b) indeed confirm the prediction that the period-doubled orbit has a larger average amplitude than the primitive one, thus indicating the importance of the bifurcated orbit V2. It should be noted that the spectrum was not resolved to the point of distinguishing the stable period-doubled orbit from the second repetition of the unstable vertical orbit. Of course, it would be worthwhile to determine the Fourier amplitudes of the spectrum, for narrow energy windows, as a function of the center of the window. However, though we can discern the broadened peaks for V and V2 (Fig. 5) the amplitudes were found to fluctuate erratically. A consistent picture of the energy evolution of the oscillations requires that the spectrum be obtained for considerably smaller value of Planck's constant, so that the density of states within each oscillation exhibits less fluctuation. We hope to be able to reveal the detailed behavior of the orbit amplitude as a function of the energy in future calculations.

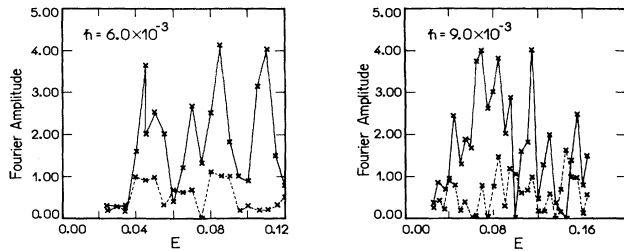


FIG. 5. Fourier amplitude, as a function of  $E$ , using Gaussian windows of width  $\Delta E = 0.05$ . The continuous line is the amplitude of V2 and the dashed line is the amplitude of V.

### III. AVERAGED WAVE INTENSITIES AND HUSIMI DISTRIBUTIONS

The classical structure, underlying the wave functions in the semiclassical limit, may be observed through the wave intensities  $|\psi_i(x, y)|^2$  and also through the Husimi [14] distributions,  $h_i(x, y, p_x, p_y)$  (a Gaussian smoothed version of the Wigner distribution).

We are interested in detecting the existence of scars due to the vertical family, and its period- $n$  bifurcations. Therefore we have calculated the state density distribution averaged over  $y$ , given by

$$\begin{aligned} \rho_i(x) &= \int |\psi_i(x, y)|^2 dy \\ &\simeq \sum_{N=0}^M \sum_{N'=0}^M \sum_{n=0}^N C_i^{n, N-n} C_i^{N'-N+n, N-n} \\ &\quad \times \phi_n(x) \phi_{N'-N+n}(x). \end{aligned} \quad (6)$$

Only even-parity states may exhibit a scar due to the vertical family as the odd-parity states are zero at the origin. Both the periodic-doubled and the period-quadrupled orbits are symmetric librations, while the period-tripled orbits are symmetric rotations (there is also a pair of period-tripled asymmetric librations which are hyperbolic).

The averaged wave intensity  $\rho_i(x)$  for the eigenstates corresponding to the eigenvalues 0.1234, 0.0401, and 0.1195 are shown in Figs. 6, 7, and 8, respectively ( $\hbar = 9.0 \times 10^{-3}$ ). The scar seen in Fig. 6 is immediately identified as due to the vertical family. The set of states exhibiting this scar are separated in energy by  $\hbar\omega_y$ . The scar seen in Fig. 7 can also be identified easily as due to the horizontal family since it belongs to a set of states that acquire a pair of oscillations as the energy is increased, the energy difference of the first two states being approximately  $2\hbar\omega_x$ . The scar seen in Fig. 8 is exhibited by a set of states separated in energy by  $\hbar\omega_y$ . To each member of this set there corresponds a member of the set exhibiting the vertical orbit scar (Fig. 6). It should be noted that, although  $\rho_i(x)$  is not specially suited to indicate the presence of periodic families other than the verti-

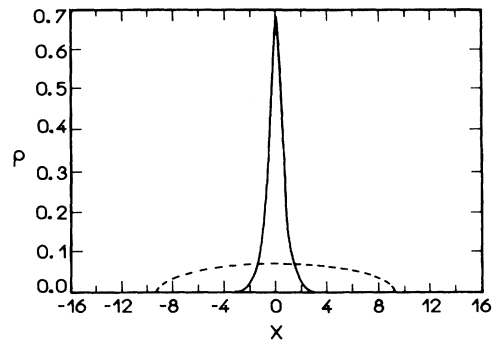


FIG. 6.  $\rho_i(x)$  for the eigenstate with  $E = 0.1234$ ,  $\hbar = 9.0 \times 10^{-3}$ . The dotted curve is the Weyl (ergodic) averaged wave intensity.

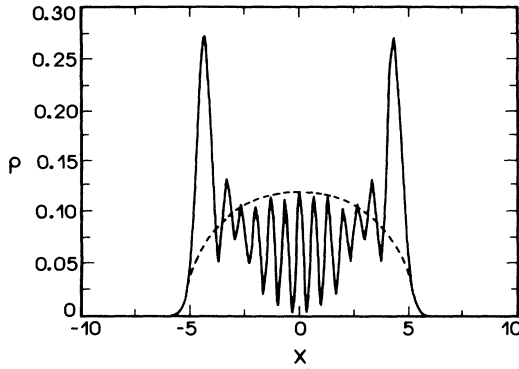


FIG. 7.  $\rho_i(x)$  for the eigenstate with  $E=0.0401$ ,  $\hbar=9.0 \times 10^{-3}$ . The dotted curve is the Weyl (ergodic) averaged wave intensity.

cal one, the plots of  $\rho_i(x)$  in Figs. 7 and 8 are important in order to compare the features of their corresponding families against the vertical family and the Weyl density.

In order to confirm the above analysis we also calculated the projected Husimi distribution for the eigenstates, as the Husimi distribution, being a function of four variables is very difficult to visualize (and to compute). The projections of  $h_i(x, y, p_x, p_y)$  on a canonically conjugate pair  $(x, p_x)$  or  $(y, p_y)$  are obtained by integrating over the other pair. Let  $|z_x\rangle$  and  $|z_y\rangle$  be the usual coherent states for the oscillators of Eq. (4), with

$$\begin{aligned} z_x &= (\sqrt{0.1}x + ip_x/\sqrt{0.1})/\sqrt{2}, \\ z_y &= (\sqrt{2}y + ip_y/\sqrt{2})/\sqrt{2}. \end{aligned} \quad (7)$$

Then, the Husimi distribution  $h_i$  can be written as

$$\begin{aligned} h_i &= |\langle \psi_i | z_x z_y \rangle|^2 \\ &\simeq \left| \sum_{N=0}^M \sum_{n=0}^N C_i^{n, N-n} \langle n | z_x \rangle \langle N-n | z_y \rangle \right|^2, \end{aligned} \quad (8)$$

where

$$\langle n | z \rangle = (z/\hbar)^n \exp(-zz^*/2\hbar)/\sqrt{n!}. \quad (9)$$

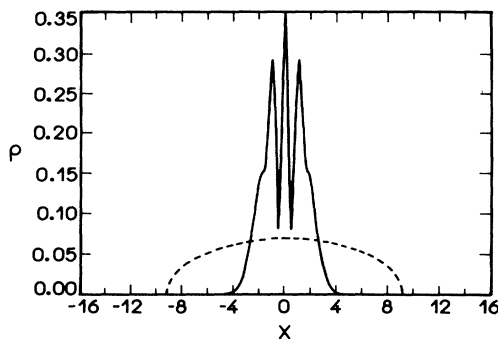


FIG. 8.  $\rho_i(x)$  for the eigenstate with  $E=0.1195$ ,  $\hbar=9.0 \times 10^{-3}$ . The dotted curve is the Weyl (ergodic) averaged wave intensity.

The projection of  $h_i$  on the plane  $(x, p_x)$  is given by

$$h_i(z_x) = \sum_{N=0}^M \left| \sum_{n=0}^{M-N} C_i^{n, N-n} \langle n | z_x \rangle \right|^2. \quad (10)$$

The projection of the plane  $(y, p_y)$  is given by a similar expression.

The projections  $h(z_x)$  and  $h(z_y)$  were calculated for a large number of eigenstates. For the eigenstates exhibiting the scar shown in Fig. 6, the Husimi projection  $h(z_x)$

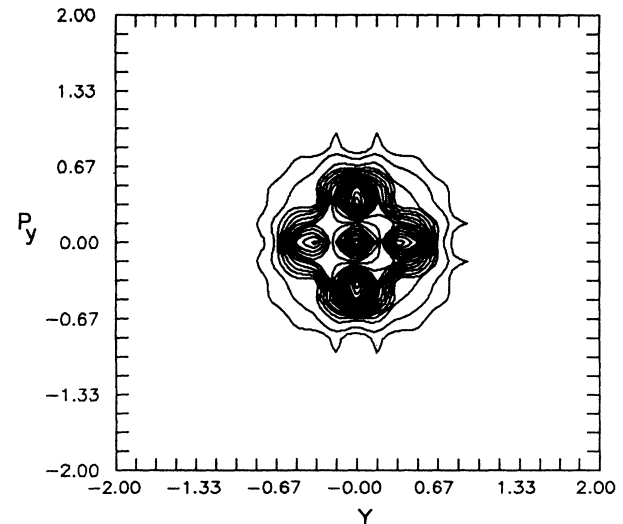
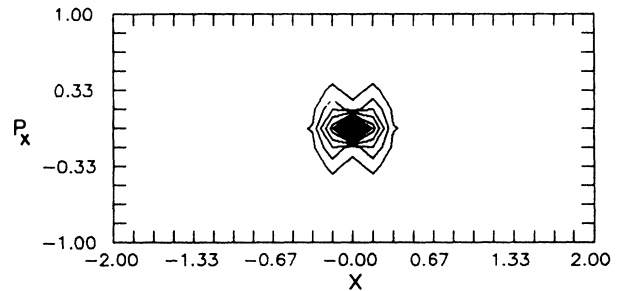
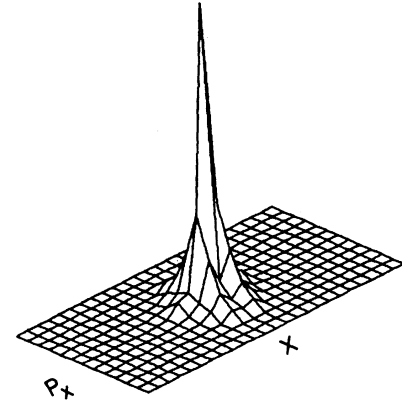


FIG. 9. The Husimi projections  $h_i(z_x)$  and  $h_i(z_y)$  for the state in Fig. 6.

(Fig. 9) has a single, narrow, peak at the origin. For the eigenstates exhibiting the scar shown in Fig. 8, the Husimi projection  $h(z_x)$  also has a single (broader) peak at the origin (Fig. 10). Now, for the former type of eigenstates, the Husimi projection  $h(z_y)$  exhibits peaks along the  $y$  axis only (see Fig. 9), while for the latter type of eigenstates, it also exhibits peaks away from the  $y$  axis (see Fig. 10), indicating that this set of states has some quanta (an even number, due to the  $x \leftrightarrow -x$  symmetry) in

the horizontal direction (remember that classically the orbit is a horizontal oscillation only at very low energies). In Fig. 11 we display the projected Husimi distributions for the eigenstate whose wave intensity is shown in Fig. 7 (horizontal family).

Following Mahoney [15], we associate with each pair of eigenstates  $n, n'$  a period and a mean energy, defined as

$$\tau_{n,n'} = k 2\pi\hbar / |E_n - E_{n'}|, \quad e_{n,n'} = (E_n + E_{n'})/2, \quad (11)$$

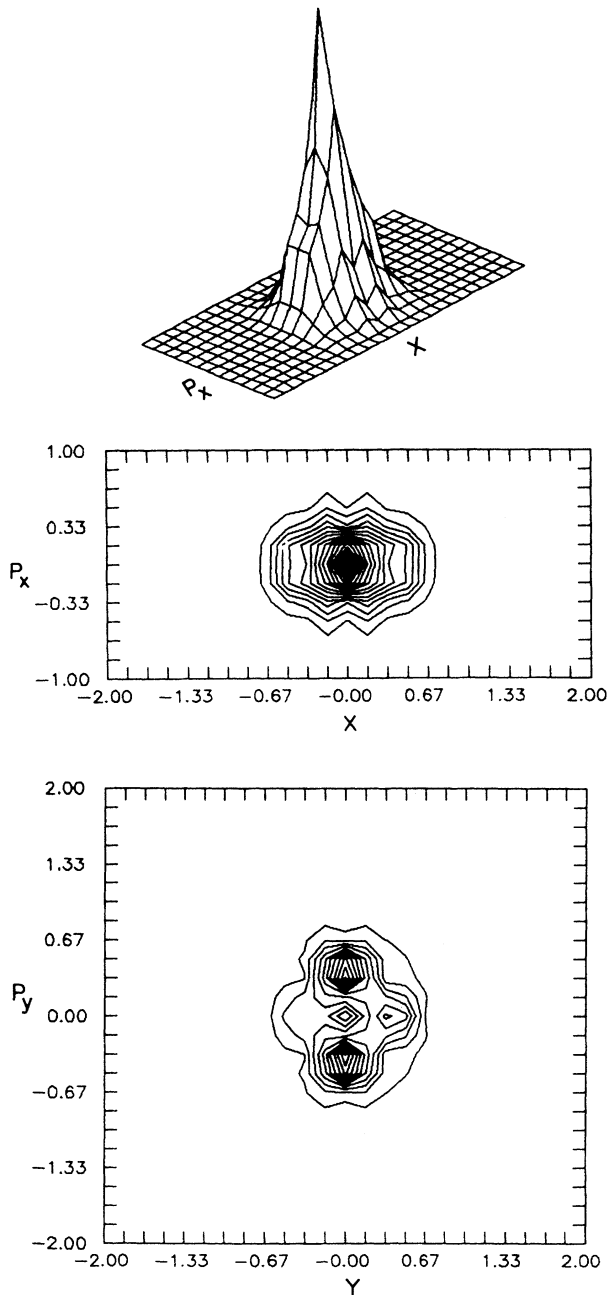


FIG. 10. The Husimi projections  $h_i(z_x)$  and  $h_i(z_y)$  for the state in Fig. 8.

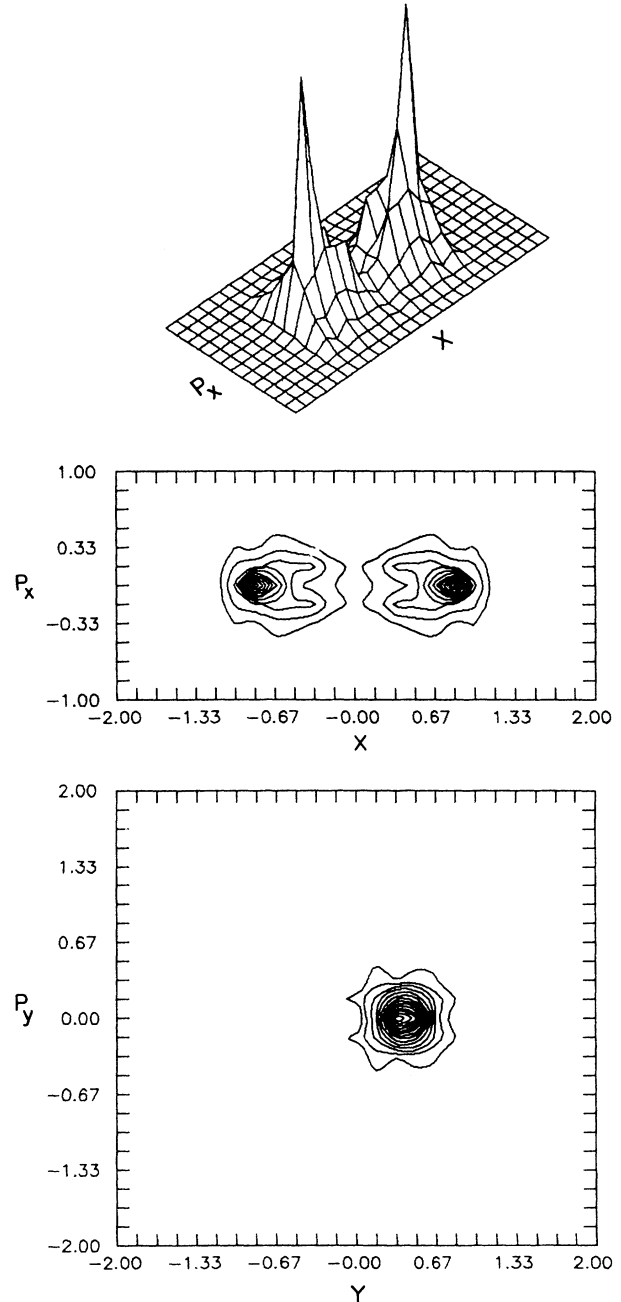
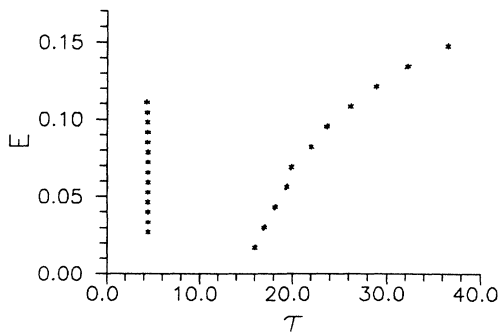


FIG. 11. The Husimi projections  $h_i(z_x)$  and  $h_i(z_y)$  for the state in Fig. 7.

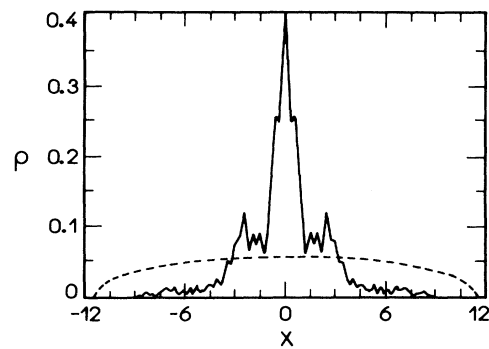
FIG. 12.  $E$ - $\tau$  plots (see description in the text).

respectively. We may then construct  $E$ - $\tau$  plots as in the classical case [8,16]. In Fig. 12 we display the  $E_{n,n+1}$ - $\tau_{n,n+1}$  plot ( $k=1$ ) for the set of states exhibiting the scar of the V family (Fig. 6). These points lie on the vertical line  $\tau=(2\pi\omega_y)^{-1}$ , which is the (classical)  $E$ - $\tau$  plot of the V family. Notice that, although the Gutzwiller trace formula predicts an energy level whenever a stable periodic orbit “quantizes,” the family of eigenstates associated with the V family remains unaffected into the unstable regions. In Fig. 12 we also display the  $E_{n,n}$ - $\tau_{n,n}$  plot ( $k=2$ ) associated with the energy separation between the states in the set above and the corresponding state in the set characterized by the scar shown in Fig. 8 (points on the other curve). The continuous curve that would fit these points has approximately the same slope of the  $E$ - $\tau$  plot of the (classical) horizontal family [8], but would lie above it. The  $E_{n,n+1}$ - $\tau_{n,n+1}$  plot for the set of states exhibiting the scar of the horizontal family (Fig. 7) lies closer to the classical horizontal family plot, but does not coincide with it. It should be mentioned that this plot tends to the classical one as  $\hbar$  gets smaller.

#### IV. FINAL DISCUSSION

In the previous work of Malta and Ozorio de Almeida [10], all attention was directed at the effect, on the spectrum, of the first iteration of the shortest periodic orbit. The above results extend our view to higher iterations and their bifurcation resonances. The computational difficulty that arises is that the number of levels within these higher frequency oscillations of the spectrum is smaller, so that even Gaussian smoothing may become unreliable. This difficulty prevents, in particular, the comparative analysis of the contribution of each periodic family to  $d_{\text{osc}}(E)$  as a function of the energy, as shown in Fig. 5. Fortunately, the peak at  $2/(\hbar\omega_y)$ , shown in the single window analysis [Figs. 3(a) and 3(b)], is sufficiently pronounced to strongly indicate the importance of the contribution of the bifurcated orbit V2.

It is not only in the analysis of the spectrum that it is

FIG. 13.  $\rho(x)$  for an eigenstate in the chaotic region ( $E=0.1861$ ), well above the period-doubling bifurcation ( $\hbar=9.0\times 10^{-3}$ ).

important to understand the features due to the classical bifurcations, which are avoided in the common use of homogeneous Hamiltonians. In the scarred states, the important qualitative features may be traced to different origins within the regular region at low energies. Thus we find that the sequence of states corresponding to the vertical orbit (Fig. 6), with only zero-point horizontal oscillation, survive neatly into the unstable region with no qualitative change in shape (confirming a previous private communication of Leboeuf and Saraceno). This is not the case of the next symmetric sequence of states (two horizontal quanta, scar of the type shown in Fig. 8). Though there is still a regular sequence in the chaotic region, with the wave intensity more spread out than in the proper scars (Fig. 8), the peak at the periodic orbit grows at the expense of the other maxima, while becoming thinner (Fig. 13). We can thus understand, at times bewildering, the number of “scarred states” as originating in torus states, as some bifurcation parameter is varied. The concentration of the states at the periodic orbit, while maintaining a spread around it, is compatible with the hypothesis of homoclinic quantization proposed by Ozorio de Almeida [17]. For  $\hbar=6.0\times 10^{-3}$ , the picture is the same and, besides, because  $\hbar$  is smaller, the scars are more neat and there are other symmetric sequences corresponding to four and six horizontal quanta.

#### ACKNOWLEDGMENTS

We acknowledge partial financial support of Conselho Nacional de Desenvolvimento Científico e Tecnológico. M.A.M.A. and A.M.O.A. are also partly supported by FINEP and FAPESP. C.P.M. acknowledges the kind hospitality of the MIT Center for Theoretical Physics, especially Professor Michel Baranger and Professor John Negele. This work was partially supported by the U.S. Department of Energy under Contract No. DE-AC02-76ER03069.

- [1] M. C. Gutzwiller, J. Math. Phys. **8**, 1979 (1971).
- [2] E. J. Heller, Phys. Rev. Lett. **53**, 1515 (1984).
- [3] E. J. Heller, in *Quantum Chaos and Statistical Nuclear Physics*, edited by T. H. Seligman and H. Nishioka, Lecture Notes in Physics Vol. 273 (Springer, Berlin, 1986), p. 162.
- [4] E. Bogomolny, Physica D **31**, 169 (1988).
- [5] M. Berry, Proc. R. Soc. London Ser. A **423**, 219 (1989).
- [6] M. Berry, Proc. R. Soc. London Ser. A **349**, 101 (1976).
- [7] R. Balian and C. Bloch, Ann. Phys. (N.Y.) **85**, 514 (1974).
- [8] M. Baranger and K. T. R. Davies, Ann. Phys. (N.Y.) **177**, 330 (1987).
- [9] M. A. M. de Aguiar and C. P. Malta, Physica D **30**, 413 (1988).
- [10] C. P. Malta and A. M. Ozorio de Almeida, J. Phys. A **23**, 4137 (1990).
- [11] Frederic J. Harris, Proc. IEEE **66**, 51 (1978).
- [12] M. Berry, *Chaotic Behavior of Deterministic Systems* 1981, Les Houches Lectures, Session 36, edited by G. Ioss, R. G. Helleman, and R. Stora (North-Holland, Amsterdam, 1981), p. 171.
- [13] A. M. Ozorio de Almeida and J. H. Hannay, J. Phys. A **20**, 5873 (1987).
- [14] K. Husimi, Proc. Phys. Math Soc. Jpn. **22**, 264 (1940).
- [15] J. H. Mahoney, Ph.D. thesis, MIT, 1987.
- [16] M. A. M. de Aguiar, C. P. Malta, M. Baranger, and K. T. R. Davies, Ann. Phys. (N.Y.) **180**, 167 (1987).
- [17] A. M. Ozorio de Almeida, Nonlinearity **2**, 519 (1989).